Models for Quantum Effects in Electron Transfer: $Co(Cp)_2^+|V(CO)_6^-$

Kenneth G. Spears* and Hairong Shang

Northwestern University, Chemistry Department, Evanston, Illinois 60208

Received: September 23, 1999; In Final Form: January 10, 2000

We model the absolute electron transfer (ET) rate and the vibrational quantum effects on ET rate previously observed experimentally for the ion pair complex $Co(Cp)_2^+|V(CO)_6^-$. We find that the absolute rate and vibrational rate effects cannot be predicted by the standard ET methods. In this work we analyze new resonance Raman, absorption, and infrared spectra and combine these results with density functional (DFT) quantum calculations of structure, vibrational modes, and solvent effects to predict absolute electron-transfer rates and vibrational quantum effects for ET. Related DFT calculations on $Na^+|V(CO)_6^-$ are used to support a spectroscopic identification of the ion pair geometry. The ET is from the radical pair state reached by charge-transfer absorption of the ion pair $Co(Cp)_2^+|V(CO)_6^-$. The weak coupling rate model based on the golden rule model of ET predicts absolute ET rates that are 135 times too large. From our DFT calculations on $Co(Cp)_2|V(CO)_6$ we conclude that a small Jahn−Teller geometry change in both radicals can reduce the orbital overlap and electronic coupling in the radical pair state so that the effective coupling matrix element is much smaller than the 417 cm^{-1} inferred from the absorption spectrum. A new study of the electronic coupling versus geometry is required to test this suggestion versus the possibility that the weak coupling model is inappropriate for our molecule. The standard model, which emphasizes totally symmetric vibrations, also cannot explain prior experimental ET rates for quantum populations ($v = 0, 1, 2$) in the nontotally symmetric CO stretching mode. These rate effects likely involve a fast IVR conversion from totally symmetric vibrations to IR active CO stretching motions followed by ET. The vibrational quantum effect on ET probably is caused by a breakdown in the Condon approximation, where an increase in the quantum number of vibration increases the electronic coupling matrix element. The models suggest a number of new experiments to probe the mechanism of ET in weak coupled molecules.

I. Introduction

A large number of review articles[1−5] on electron transfer have been published, and we refer to those works for a more complete introduction. Many theoretical and experimental results have shown that molecular electron transfer (ET) has control elements from electronic interactions, geometric changes, and environmental response. However, these multiple mechanistic elements make it difficult to test theoretical models of ET with experiments. We have experimentally shown that *ET rates can be quite dependent on the vibrational quantum state* in solutions at room temperature,[6] and in this manuscript we examine how such data can provide an additional test for geometric reorganization and electronic coupling components of the ET rates. *Therefore, our objective is to analyze new data on resonance Raman, absorption, and infrared spectra and combine these results with quantum mechanical molecular models and rate models to predict absolute ET rates and vibrational quantum effects for ET in the ion pair* $Co(Cp)_2^+|V(CO)_6^-$. We show that the normal assumptions used in interpreting ET with these types of data are not adequate to explain the observed rates. The absolute rate prediction is 135 times larger than observed, and we conjecture that small geometry changes between states greatly affect the electronic coupling magnitude. The experimental vibrational quantum dependence of the ET rate in an IR active mode is not explainable in the standard model, which emphasizes totally symmetric vibrational modes. We conjecture that electronic-vibrational coupling (Condon breakdown) creates vibrational quantum effects on the ET rates.

The ion pair $Co(Cp)_2^+|V(CO)_6^-$ exists at high concentrations in low-dielectric-constant solvents. The electronic interaction of the metal centers through the ligand overlap creates a charge-transfer absorption band with low extinction coefficient near 620 nm and a very broad bandwidth having no vibrational structure. These features imply a weak coupling of the ion pair to an uncharged radical pair state that can be populated by charge-transfer absorption. The CO stretching modes of the vanadium carbonyl are decoupled from the other vibrations so that these modes do not relax by intermolecular relaxation processes on the nominal 1−2 ps time scale of the lower frequency vibrations. Therefore, our prior experiments with transient infrared absorption[6] were able to measure ET rates for vibrational quantum numbers 0, 1, and 2 in the infrared active CO stretching mode. The respective time constants for these quantum levels were 26.4, 11.3, and 5.5 ps, and the ground state recovery kinetics showed rise times consistent with these time constants. These quantum results show an unusual sensitivity of ET rate to an infrared active vibration rather than totally symmetric vibrations. *In addition, our earlier models*[7] *demonstrated that details of vibrational displacements are very important for controlling ET in molecules that have one or two modes whose individual reorganization energies are a large fraction of the total vibrational reorganization energy in the molecule. This is important to emphasize*, and one should not overgeneralize[8] a common case, where the vibrational reorga-

* Corresponding author. E-mail: k-spears@nwu.edu.

10.1021/jp993405i CCC: $19.00
Published on Web 03/04/2000

nization energy is more uniformly distributed over a large number of vibrations.[9]

The prediction of ET rates requires both theoretical models and spectroscopy data. We use ab initio density functional theory (DFT) calculations to define the geometry of the ion and radical pair in gas phase and solution. Fortunately, we find that only two structures are likely for this ion pair, and experimental data support the lowest energy structure. The DFT models yield good representations of the vibrations and bond length changes in ionic and neutral radical molecules. *In contrast to many ET problems that involve excited electronic states, this particular problem only involves computations for the lowest electronic states of the relevant components.* Solvent reorganization energy is estimated from theoretical solvent continuum models with volumes defined by an isodensity surface. The absorption spectrum provides an estimate for the electronic coupling via the usual perturbation models[10] and also serves as a self-consistency check on resonance Raman models and reorganization energy models. The simplest ET rate model has direct electronic coupling and a sum over Franck−Condon factors (FCF). As shown previously,[7] this simple model can show a quantum dependence of ET rate from the FCF contribution to the model.

The computational results described in this manuscript focus on the ion pair and solvation components of the problem that are required to predict ET rates. A later manuscript[11] will discuss the DFT computational modeling for radicals in more detail.

II. Experimental Results

A. Compound Synthesis and Handling. The $Co(Cp)_2^+|V(CO)_6^-$ ion pair was synthesized through the reaction of $Na^+|V(CO)_6^-$ and $Co(Cp)_2^+|PF_6^-$ by an air-free method described previously.[12] It is important to use freshly distilled solvent and air-free handling with drying under nitrogen for about 12 h. The final product was identified by UV−vis and IR spectra in methylene chloride (CH_2Cl_2). Since neither $Co(Cp)_2^+$ free cation nor $V(CO)_6^-$ free anion has absorption in visible region,[12] the UV−vis spectrum is a good identification method for the ion pair complex. The Raman spectroscopy measurements used septa-sealed NMR tubes under nitrogen with freshly distilled solvent. The ion pair did not demonstrate decomposition effects during Raman experiments, although solvent impurities and dissolved air will cause decomposition.

B. Absorption Spectra. Routine UV−vis spectra were collected by a diode array spectrophotometer (HP 8452A) with a resolution of 2 nm, while more complete spectra in the near-IR were measured by an Olis-modified Cary 14 spectrometer with a resolution of 1 nm.

Figure 1a shows the absorption spectra in the visible region (the charge-transfer band) of the $Co(Cp)_2^+|V(CO)_6^-$ ion pair in dichloromethane (DCM) and tetrahydrofuran (THF) solvent at room temperature. These spectra are similar to those reported previously.[12] For DCM solutions at very high concentrations, the peak seems to make a slight blue shift, suggesting the possibility of higher agglomeration. When the concentration is higher than 15 mM, the peak is around 601 nm, at lower concentrations the peak is around 620 nm. By plotting the maximum extinction in the absorption spectra versus concentration (shown in Figure 1b), we compute the equilibrium constant and derive an extinction coefficient for this charge-transfer transition. Unfortunately, the curvature is extremely slight in this concentration range so that any fitting is very sensitive to errors in the extinction coefficient due to the uncertainties of baseline subtraction, slight peak shifts, and concentration errors.

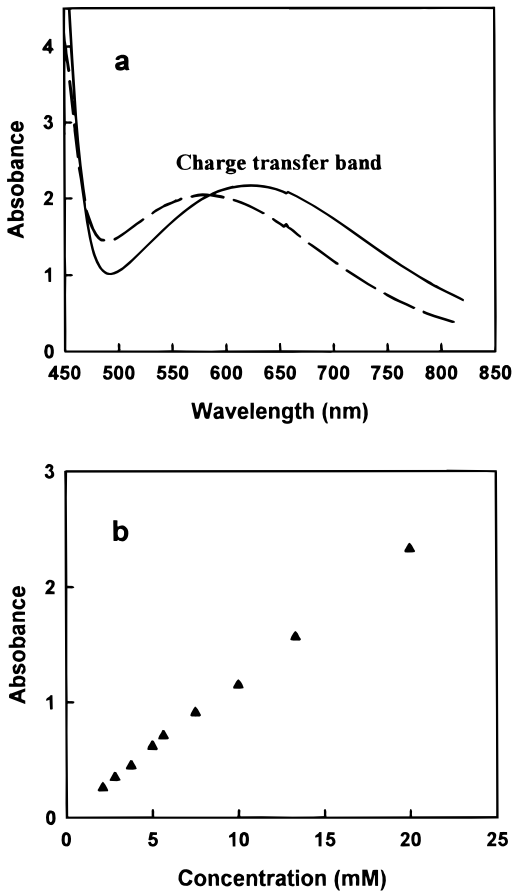

Figure 1. (a) Absorption spectra of the $Co(Cp)_2^+|V(CO)_6^-$ ion pair dissolved in CH_2Cl_2 (DCM) and tetrahydrofuran (THF). The solid line represents the DCM solution ($\lambda_{max} = 616$ nm); the dashed line represents the THF solution ($\lambda_{max} = 582$ nm). (b) Absorbance of the ion pair in the DCM solution versus the total concentration of the ion pair.

We find that the equilibrium constant for this ion pair formation in DCM solution is 3600 M^{-1}, and the maximum extinction coefficient is 125 ± 15 M^{-1} cm^{-1}, where the error is a rough estimate of effects based on a variety of simulations of errors in the baseline. If we apply the Hush model[10] of weak coupling for the metal-to-metal charge-transfer (MMCT) transitions, the electronic coupling via eq II.1 is estimated as 417 ± 50 cm^{-1}.

$$H_{rp} = \frac{2.06 \times 10^{-2}}{R}(\epsilon_{max}\bar{\nu}_{max}\Delta\bar{\nu}_{1/2})^{1/2} \qquad \text{(II.1)}$$

In this formula R is the ET distance in angstroms, ϵ_{max} is the molar extinction coefficient (M^{-1} cm^{-1}), $\bar{\nu}_{max}$ is the transition maximum (in cm^{-1}) of 16 234 cm^{-1} for this ion pair, and $\Delta\bar{\nu}_{1/2}$ is the bandwidth (in cm^{-1}) at half-height, 7038 cm^{-1} for this ion pair. The ET distance is chosen as the equilibrium distance between V and Co of the ion pair in the DCM solution, 5.9 Å. The coupling value of 417 cm^{-1} is at the upper limit of what is considered a weak coupling model. The calculated (see later discussion) dipole moment for the ion pair is 26.7 D in solution, while the estimated point charge value using an R of 5.9 Å is 28.3 D.

C. Resonance Raman Spectra. The Raman spectra of the ion pair and each of the ions were obtained with many excitation wavelengths throughout the region of charge-transfer absorption. The Raman instrument is a JY triple spectrometer (Spex 1877) with a liquid nitrogen cooled CCD detector on the dispersion stage. The gratings were blazed at 750 nm and the dual-grating, subtractive dispersion prefilter was adjusted to minimize scatter

TABLE 1: Raman Spectra for the $Co(Cp)_2^+|V(CO)_6^-$ Ion Pair (IP) and Free Ions

vibrational mode[a]	$Co(Cp)_2^+$ [b] (cm^{-1})	$V(CO)_6^-$ [c] (cm^{-1})	IP[d] (cm^{-1})	D[e] DCM	D[e] THF
υ_4', Co−Cp str (A_{1g})	315		315	0.51	0.23
υ_{16}', Cp ring tilt (E_g)	383		383	0.33	0.23
υ_3', Cp ring breath (A_{1g})	1109		1109	∼0	∼0
υ_2, V−C str (A_{1g})		373	373	0.03	0.12
υ_4, V−C str (E_g)		393	392	0.49	0.72
υ_3, C−O str (E_g)		1894	1894	0.73	1.03
υ_1, C−O str (A_{1g})		2020	2020	0.26	0.29

[a] Prime is for $Co(Cp)_2^+$, and unprime is for $V(CO)_6^-$; error in υ is ± 1 cm^{-1}. [b] $Co(Cp)_2^+PF_6^-$ was dissolved in acetone. [c] $Na^+V(CO)_6^-$ was dissolved in DCM; diglyme was in the initial salt for stabilization. [d] Ion pair was dissolved in DCM. [e] $D = I_{perpendicular}/I_{parellel}$ is the depolarization ratio for the ion pair solutions;. $I_{perpendicular}$ is the Raman intensity with polarization perpendicular to the laser polarization, and $I_{parallel}$ is parallel to the laser polarization. Solutions of ion pair in dichloromethane (DCM) and tetrahydrofuran (THF).

for a desired spectral width. The excitation and collection optics were in a backscattering geometry, and a camera lens was used for light collection and collimated transfer into an achromatic focusing lens and polarization scrambler. A simple thin film polarizer was used to determine polarization ratios. The spectrometer light transmission was calibrated with a reference lamp and opaque diffusing plate that allowed correction for transmission and CCD sensitivity versus wavelength. The exciting laser was either an argon ion (Coherent Innova 400) pumped dye laser (Spectra Physics 3500) or a titanium sapphire laser (Spectra Physics Tsunami) operated CW. The Raman scattering intensity from solutions of the compound was weak. We operated at concentrations of about 15 mM for the ion pair and 30 mM for salts of the individual ions in the ion pair (free ions). The solutions were prepared with 2.5% of a deuterium isotope mixture of CD_2Cl_2 when dichloromethane (DCM) was used as the solvent. The C−D band at 2200 cm^{-1} and other solvent bands served as internal standards. Since $Co(Cp)_2^+|PF_6^-$ is hard to dissolve in DCM or THF, the Raman spectrum of this compound was measured in acetone. Acetone has a relatively broad Raman speak at 390 cm^{-1}, which overlaps with the ring-tilt vibration (384 cm^{-1}) of $Co(Cp)_2^+$. The solvent background was subtracted by normalizing to nearby solvent peaks. The Raman spectra of the free $V(CO)_6^-$ ion was taken in both DCM and acetone with the $Na^+(diglyme)_2$ stabilizer provided by the supplier (Strem Chemicals).

The observed Raman peaks and depolarization of the ion pair and free ion are summarized in Table 1, and some spectra are shown in Figure 2. The vibrational frequency difference between $V(CO)_6^-$ free ion in DCM (dielectric constant, $\epsilon = 8.93$) and in higher polarity acetone ($\epsilon = 23$) is within 1 cm^{-1}, and the vibrational frequencies of the $Co(Cp)_2^+$ cation and $V(CO)_6^-$ anion are consistent with previous reports, which used solutions of H_2O[13] and acetonitrile,[14] respectively. Table 1 shows that there is little frequency change between free ions and the ion pair.

The depolarization ratios of the ion pair and free ion vibrations are similar, except for the totally symmetric υ_1 mode. For this mode the depolarization ratio of the ion pair was 0.26, while the free ion gave a low depolarization ratio of 0.01. The latter value indicates that the υ_1 mode in the free ion is well polarized, as expected for an octahedral ion. A change in depolarization ratio without a detectable change in frequency suggests that there is slight distortion of $V(CO)_6^-$ in the ion pair.

The Raman intensity of the totally symmetric mode, υ_1, was significantly enhanced, but most other vibrations were not

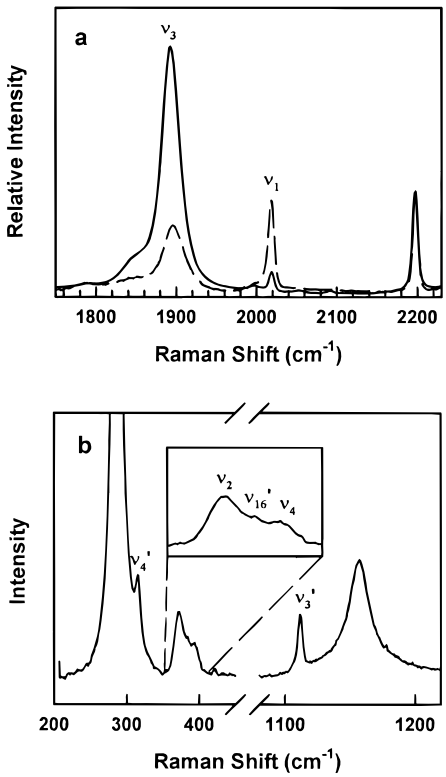

Figure 2. (a) Raman spectra of the ion pair and free $V(CO)_6^-$ ion in DCM solution in the CO stretch region where the solid line is the free ion and the dash line is the ion pair. (b) Raman spectrum of the ion pair in DCM solution in the low-frequency region. The vibrations belonging to the compound are assigned in the figures; the unassigned peaks are from the solvent scattering.

enhanced or minimally enhanced. The comparison of free $V(CO)_6^-$ and the ion pair for the 2000 cm^{-1} region is shown in Figure 2a. Here we show the large enhancement of υ_1, the A_{1g} mode at 2020 cm^{-1}, versus mode υ_3, the E_g mode at 1894 cm^{-1}. In Figure 2a, the two spectra were obtained at the same excitation wavelength of 590 nm and are not normalized. The low-frequency region is shown in Figure 2b, where we have modes from both species in the ion pair. The integrated intensities of different vibrations were obtained by fitting the Raman peaks and integrating and normalizing to the nearby solvent peak. These raw intensities were then corrected by a spectrometer transmission calibration. For the high-frequency region the Raman peaks were normalized to the 2200 cm^{-1} peak (totally symmetric C−D stretch in CD_2Cl_2); for the low-frequency region the Raman peaks were normalized to a strong solvent band at 285 cm^{-1}.

The best method for obtaining absolute Raman enhancements is to compare resonance Raman with nonresonance excitation wavelengths. However, the broad absorption band in the visible prevents such a comparison so an approximate calibration procedure was used to estimate the absolute Raman enhancements of the ion pair relative to the free ion. The relative concentration of $V(CO)_6^-$ in the two Raman experiments is obtained by absorbance spectra comparisons at 400 nm. A 100 times dilution of both solutions is used in the absorption spectrometer, and this dilution also changes the ion pair equilibrium concentration to nearly free ions. Free $V(CO)_6^-$ has no absorption in the visible region, while it has very strong absorption below 400 nm that also overlaps with absorption transitions of $Co(Cp)_2^+$. This method gives approximate enhancements, where about 10% measurement uncertainty arises from errors in correcting for equilibrium and the overlapping

absorption bands. *A more fundamental uncertainty arises from assuming that the distortion in the ion pair does not change the relative intensities of different vibrations.* Raman spectra of the ion pair and free $V(CO)_6^-$ ion in DCM solution were obtained at many excitation wavelengths in the charge-transfer band region of the ion pair. We found that at all excitation wavelengths the absolute resonance Raman enhancement of υ_2, υ_3, and υ_4 in the ion pair, when compared with $V(CO)_6^-$, was about 0.5, while υ_1 was about 14. The enhancement of 0.5 rather than 1.0 or greater suggests that distortion of $V(CO)_6^-$ in the ion pair is changing the relative intensities of modes. An alternative explanation is Raman de-enhancement, which is present from interference with a higher energy state accessed via its weak absorption tail extending in the charge-transfer band absorption. This phenomenon is well-known[15,16] and could become an issue with weak extinction transitions. The excitation wavelength dependence of the data is noisy, but all wavelengths have broad featureless enhancements; for example, the wavelength scan of υ_1 enhancement is also noisy, but it has a broad peak around 630 nm, which is consistent with the absorption spectrum. Since υ_1 is the only strongly resonant mode and it has a broad excitation spectrum with a peak similar to the charge-transfer band, we assume that the ratio values of 0.5 are more affected by the distortion in the ion pair than by interference effects with higher states.

As we discuss below, the relative resonance enhancement is conveniently used in fitting the absorption spectrum of the ion pair. Therefore, we compare the relative intensities within the ion pair to infer an enhancement of υ_1, υ_4, and υ_3. Since we must ultimately normalize the intensity relative to one frequency, we scale the data via an arbitrary setting of the absolute enhancement of υ_2 equal to unity. With this procedure, the relative enhancements of υ_3 and υ_4 are close to unity, and the relative enhancement of υ_1 at different excitation wavelengths from 580 to 680 nm in the charge-transfer band shows an average relative enhancement of 28. More precisely, by averaging over many excitation wavelengths and setting the υ_2 mode at unity enhancement, the average enhancements of υ_4, υ_3, and υ_1 relative to υ_2 are 1.06, 1.15, and 28, respectively. As we discuss later in our use of this information, these values serve to confirm our theoretical modeling of displacements rather than provide the sole definition of vibrational displacements.

Since $Co(Cp)_2^+|PF_6^-$ is hard to dissolve in DCM or THF, the Raman scattering of the vibrations from $Co(Cp)_2^+$ species is not directly available for comparison with the IP. However, if we use a starting hypothesis that only totally symmetric modes with large displacement are greatly enhanced in most resonance Raman spectra, we find a small enhancement of 1.3 for the Co−Cp stretch vibration υ_4' from its relative intensity to the nontotally symmetric ring-tilt υ_{16}'. Calculations discussed later suggest little geometry change of the Cp ring between the two structures $Co(Cp)_2^+$ and $Co(Cp)_2$, which supports the idea that enhancement of the totally symmetric ring breathing vibration, υ_3', is quite small. This method provides an estimate of 1.7 for the enhancement of υ_4' from its intensity relative to υ_3'. Since υ_4' in DCM solutions is a shoulder of the strong solvent peak at 285 cm^{-1}, we sought to check the enhancement factors by studies in THF. Solutions in THF have very weak Raman scattering below 500 cm^{-1} and the line widths are also narrower, which makes the overlapping regions clearer. However, the $Co(Cp)_2^+|PF_6^-$ could not be dissolved at high concentration in THF so that acetone solutions had to be used for the free ion reference. The relative intensity of υ_4' to υ_3' for the ion pair in THF solution is 1.5 times as strong as it was for the $Co(Cp)_2^+$ free ion dissolved in acetone, and the relative intensity of υ_4' to υ_{16}' from the ion pair in THF solution is about 1.3 times as strong as it was for the $Co(Cp)_2^+$ free ion dissolved in acetone. From these different comparisons we conclude that there is enhancement of υ_4' with an absolute value that could be from 1.3 to 1.7.

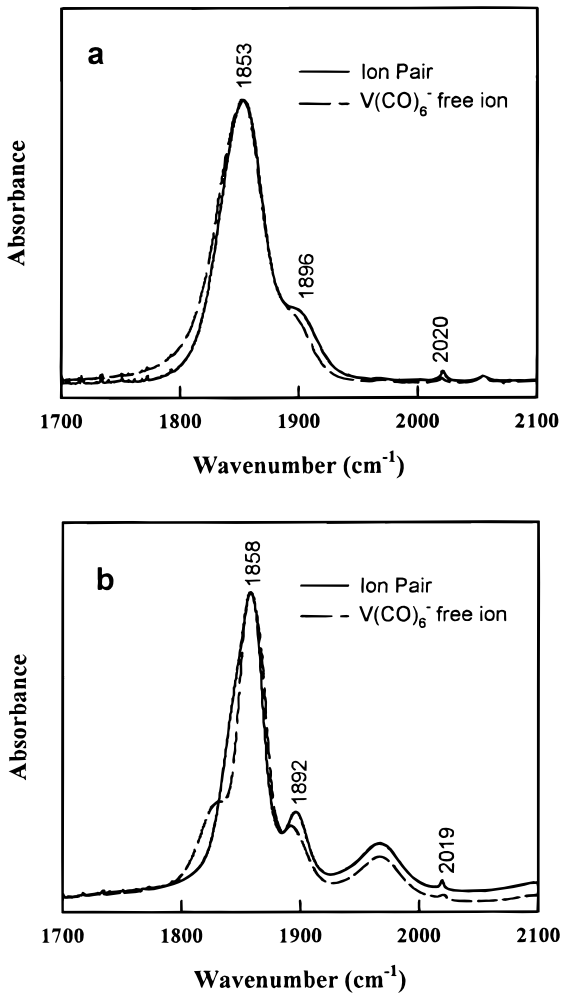

Figure 3. (a) FT-IR spectra of the ion pair and free $V(CO)_6^-$ ion in DCM solution. (b) FT-IR spectra of ion pair and free $V(CO)_6^-$ ion in THF solution. The spectrometer resolution was 0.5 cm^{-1}.

D. Infrared Spectra. The FT-IR spectra of the ion pair and free $V(CO)_6^-$ ion in DCM are shown in Figure 3a with a resolution of 0.5 cm^{-1}; they were obtained with a BIO-RAD (FTS-60) spectrometer. Spectra in solutions of THF and acetone are shown in Figure 3b. To keep the ion pair in solution and avoid saturation of IR intensity, 0.025 mm thin IR-cells were used with CaF_2 windows. Three CO stretch vibration modes were observed in both the ion pair and free $V(CO)_6^-$ ion: υ_6 (T_{1u}, 1854 cm^{-1}), υ_3 (E_g, 1894 cm^{-1}), and υ_1 (A_{1g}, 2020 cm^{-1}), the first one is IR active, the last two are Raman active. The frequency difference between the ion pair and free $V(CO)_6^-$ ion is within 1 cm^{-1}. The frequency of the IR active CO stretch in DCM, THF, and acetone is 1853, 1858, and 1859 cm^{-1}, respectively. These values are consistent with the published results, which show values within 3 cm^{-1} of 1856 cm^{-1} for many solvents except halogen containing methanes.[14] The line-widths of the υ_6 mode in THF and acetone are essentially the same value of 21 cm^{-1}, while in DCM they broaden to 45 cm^{-1}. The greater line-width and frequency shift are probably due to the interaction between compound and solvent, especially the chlorides. These line width effects are also observed in Raman

spectra. In DCM, the Raman line widths of υ_1 (2020 cm^{-1}, A_{1g}) and υ_3 (1894 cm^{-1}, E_g) are 6 and 30 cm^{-1} for the ion pair and 6 and 25 cm^{-1} for free $V(CO)_6^-$. In THF solution, the line widths of υ_1 and υ_3 for the ion pair are 6 and 18 cm^{-1}, respectively. In the ion pair there is a slight splitting of υ_3 in the high-frequency side with a shoulder around 1910 cm^{-1}.

The totally symmetric CO stretch mode shows a weak IR absorption, but it is stronger for the ion pair than free $V(CO)_6^-$ ion, again indicating a geometry distortion of $V(CO)_6^-$ in the ion pair. In the free ion solution there is a low-frequency shoulder at 1828 cm^{-1} that is always proportional to concentration, and it may be associated with the diglyme component.

III. Computational Modeling

A. Structure and Vibrations of Individual Components. An earlier report from our lab[17] discussed the DFT models for $V(CO)_6^-$ and the isoelectronic $Cr(CO)_6$ in terms of the basis set, DFT method, vibrational frequencies, and charge partitioning among the atoms. The results suggested that the B3LYP method provides good results for bond lengths and vibrational frequencies. The CO stretching modes were systematically too high in frequency by amounts similar to the diatomic case of 30−60 cm^{-1}. The negative charge was shifted onto the oxygens, where the natural bond order analysis was effective at contrasting charge partitioning in the Cr and V isoelectronic species. The radical $V(CO)_6$ and its anion also have been previously modeled via the SCF−Xα−DV theoretical method.[18]

The radical $V(CO)_6$ is a relatively stable 17 electron radical, and it has been studied by EPR[19−22] and other spectroscopies.[23,24] The molecule distorts from an octahedral geometry very easily, as predicted from the Jahn−Teller theory, so that crystal packing and solvent effects make it difficult to be confident of the lowest energy structures inferred by experimental methods. Our computational results from Gaussian 94W[25] are consistent with experimental details in the broadest sense. There is a dynamic Jahn−Teller distortion possible for the isolated radical and the axis distortion is small for different symmetry distortions. We were able to find a D_{3d} symmetry as the minimum energy geometry and another local minimum of D_{2h} symmetry at 207 cm^{-1} higher energy. For the D_{2h} symmetry the vibrational frequencies had a single imaginary vibration, which indicates its instability to distortion.[11] The D_{3d} geometry is unusual in that the singly occupied A_{1g} orbital is lower in energy than the two doubly occupied E_g orbitals, which are at slightly different energies for the α and β spin systems. While subtle shifts of orbitals are possible, we have used the D_{3d} geometry as representative of the radical in modeling ion pairs. In a later section we make additional comments on structural distortion when paired with $Co(Cp)_2^+$.

The computed changes in structure between the ionic and radical forms of $Co(Cp)_2^+$ and $V(CO)_6^-$ are summarized below in Table 2. These changes are reasonably independent of basis set size for the CO bond length, but there is some sensitivity of the metal−carbon distance to basis set size and DFT method. We have performed only enough calculations for the cobalticinium molecule to allow study of the ion pair with comparable basis set accuracy. Both calculations and experiments[26] show that each Cp ring in the $Co(Cp)_2^+$ ion is a plane. An electron diffraction experiment shows that H atoms are bending inward to the cobalt atom by 3.7° in the $Co(Cp)_2$ radical[27] while retaining D_{5d} or D_{5h} symmetry.

The symmetry in calculations is D_{5d}, and the calculation shows this bending angle as smaller than the experimental results. The vibrational spectrum of the $Co(Cp)_2^+$ ion is experimentally well-known,[13] but the vibrational spectrum of the $Co(Cp)_2$ radical is not known. However, one can use estimates from the known vibrational spectrum of ferrocene,[28,29] $Fe(Cp)_2$, for estimating frequencies in the $Co(Cp)_2$ radical.

TABLE 2: Geometry Change between Free Radicals and Ions Calculated by DFT(B3LYP)[25]

	$V(CO)_6^-$	$V(CO)_6$		$Co(Cp)_2^+$	$Co(Cp)_2$
symmetry	O_h	D_{3d}		D_{5d}	D_{5d}
ΔR(C−O)[a]		−0.0172	ΔR(C−C)[a]	0.001404	
ΔR(V−C)[a]		0.0519	ΔR(C−H)[a]	−0.000544	
∠(C−V−C)[b]	180	86.3, 93.7	ΔR(Co−Cp)[a]	0.089059	
∠(O−C−V)[b]	180	179.41			
basis sets	6-311+G(d,p) for C, O 6-311G for V			6-31G* for C, H 6-311G for Co	

[a] ΔR = R(radical) − R(ion), the bond length change in angstroms. [b] The angles are in degrees. Notation for angles is ∠(ABC), where atom B is at the vertex.

TABLE 3: Vibrations for $V(CO)_6^-$ Ion and $V(CO)_6$ Radical

			$V(CO)_6^-$ (cm^{-1})		$V(CO)_6$ (cm^{-1})
symmetry	label	motion	exptl[a]	calc[b]	calc[c]
A_{1g}	ν_1	C−O str	2020	2084	A_{1g}: 2169
A_{1g}	ν_2	M−C str	374	382	A_{1g}: 349
E_g	ν_3	C−O str	1894	1974	E_g: 2045
E_g	ν_4	M−C str	393	390	E_g: 313
T_{1g}	ν_5	b-MCO		364	E_g, A_{2g}: 326, 337
T_{1u}	ν_6	C−O str	1858	1954	E_u, A_{2u}: 2066, 2069
T_{1u}	ν_7	b-MCO	650	678	E_u, A_{2u}: 622, 543
T_{1u}	ν_8	M−C str	460	462	E_u, A_{2u}: 402, 399
T_{1u}	ν_9	b-CMC		96	E_u, A_{2u}: 96, 90
T_{2g}	ν_{10}	b-MCO	517	523	E_g, A_{1g}: 471, 456
T_{2g}	ν_{11}	b-CMC	84	89	E_g, A_{1g}: 82, 83
T_{2u}	ν_{12}	b-MCO		518	E_u, A_{1u}: 456, 512
T_{2u}	ν_{13}	b-CMC		54	E_u, A_{1u}: 55, 66

[a] Experimental values in solutions from IR and Raman.[14] [b] B3LYP calculation, basis set: 6-311G(d,p) for C and O, 6-311G for V. Gaussian 98W.[33] No empirical correction was applied to computed frequencies. [c] T symmetry is split into (A,E) symmetry pairs in D_{3d} final geometry.

The vibrational spectrum of $V(CO)_6$ is not known except for the IR-active CO stretch.[30,19] The computed geometric information for the radical compares well with experiments,[31,32] and since the prior vibrational computations on the anion agree with the data[17] we expect comparable accuracy for the computed vibrational frequencies of $V(CO)_6$. In Table 3 we provide a summary of vibrational data and computed frequencies for those modes that are known for $V(CO)_6^-$ and $V(CO)_6$. Computational models for $V(CO)_6^-$ show CO stretching modes with frequency displacements of 64−96 cm^{-1}, similar to diatomic CO (+51), which is due to computational method offsets for the CO bond.

B. Structures of Ion Pairs and Radical Pairs. The ion pair computations were done with Hartree−Fock (HF) and DFT methods. In these computations the bond length coordinates of the individual ions were held fixed at the minimum computed for the individual ions. Initially, we explored many different options for possible minima between the ion pair with both semiempirical (ZINDO) and HF methods using single, double, and triple contacts. One category of stable geometry is either double contact or triple contact of the O atoms of the $V(CO)_6^-$ with the top of the cobalticinium ring. The most stable geometry in this group is a top-triple contact in the orientation where the oxygen atoms are between two hydrogen atoms in the Cp ring. Figure 4a shows this orientation with space-filling plots selected to show the atom arrangement rather than more accurate representations of size. The second geometry that we explored had side interactions nestled between the two rings of cobalticinium with either a single contact or double contact. Other

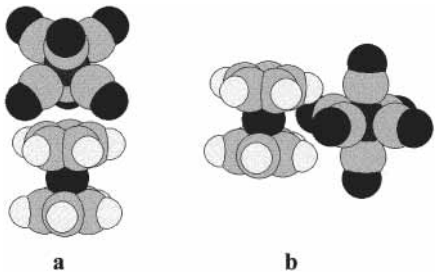

Figure 4. (a) Space-filling model of $Co(Cp)_2^+|V(CO)_6^-$ with three oxygens contacting the top of the Cp ring. (b) Space-filling model of $Co(Cp)_2^+|V(CO)_6^-$ with two oxygens contacting the cleft between the two Cp rings.

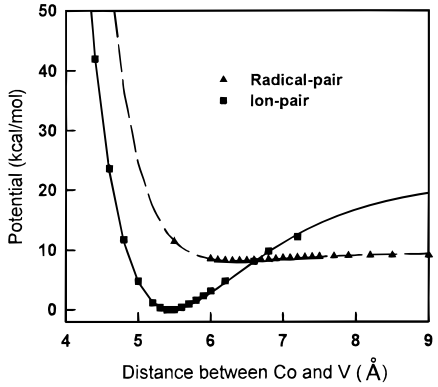

Figure 5. Gas-phase calculation of energy versus metal separation distance for the ion pair $Co(Cp)_2^+|V(CO)_6^-$ and a neutral pair in a triplet state. DFT quantum calculations for individual species were used to define a fixed geometry for each component of the pair, while the total DFT energy was computed for each metal separation distance.

cases of double contact with the ring edges (90°) were less stable. We found that the double side contact between the two rings was the most stable, and it is shown in Figure 4b. The energies calculated by HF are different from those calculated by the DFT method; however, the distances at the minimum are similar for these two methods. The DFT method gave the energies and distances at the minimum for the top-triple as −55.4 kcal/mol and 6.1 Å, while the side-double model had −63.1 kcal/mol and 5.4 Å. These energies are relative to the energy at infinite distance between the Co and V atoms. The side-double is more stable than top-triple in the gas phase by about 8 kcal/mol. For the two orientations of the ion pair shown in Figure 4 we also computed many more points of separation to define an interaction potential. The potential energy is shown in Figure 5, where the solid and dashed lines are the fitted curves of ion pair and radical pair potentials, respectively.

The radical pair computations used the DFT method and modeled the triplet state of the radical pair. We also defined a potential energy by changing the relative separation distance at fixed bond lengths for the individual radicals in the double side contact geometry, where $V(CO)_6^-$ is in the D_{3d} geometry. We note that the potential energy for the radical pair is very flat since there is little net interaction energy despite the large quadrupole and hexadecapole moments of the individual species. The energy gap between the radical pair and ion pair in the gas phase is 2870 cm^{-1}. The gas-phase dipole moments of the ion pair are 21.4 D for the top-triple and 19.8 D for the side-double structures, respectively.

C. Structures and Energies in Solvent. The methods for performing ab initio calculations in solvent are a current area of research in many groups. The polarized continuum model (PCM) of Tomasi and co-workers[34] has been modified to perform the integrals over a static isodensity surface.[35] We have used the IPCM method as implemented in the Gaussian 98W computational package[33] for our computations. This method provides a continuum result for a given dielectric constant without arbitrary selections of radii, but it still requires selection of an isodensity energy. A useful literature survey and new tests of isodensity cavity size selection in reaction field theories has been recently published.[36] Other improvements in the PCM models provide a self-consistent procedure that allows the polarizable continuum to modify the wave functions, which is often called a self-consistent reaction field (SCRF) method. SCRF methods are potentially very complex, and their assessment is an active area of research. For example, the penetration of wave functions into the solvent has been analyzed to correct for volume polarization effects in SCRF models.[37] Computations with ab initio SCRF methods are very time-consuming for large molecular systems such as our ion pair, with 34 atoms, so that we have elected to perform our analysis at the level of IPCM computations.

Fortunately, we seek a difference in energy between two molecular states, the ion pair and the radical pair, so there is an opportunity for cancelation of errors. In particular, the IPCM method will not provide accurate absolute solvation energies, but differences of solvation energy between molecular pairs that differ in their internal charge distribution are likely to be more accurate. Also, it is likely that the diffuse charge density of the solute reduces errors. There are three items that we seek for our interpretive work, the energy versus separation in each pair, the energy difference between the ion and radical pair, and the solvent reorganization energy in changing from ion pair to radical pair. We initially checked the IPCM method to define the range of solvation energies that arise from different choices of isodensity energy. The first calibration was to study the change in energy for the $V(CO)_6^-$ ion solvated in DCM at a dielectric constant, ϵ, of 8.93. Here we could vary the integration angle variables, ϕ and θ, and the isodensity value. The integration variable density may need to be larger for molecules having protrusions; for example, one group used 8040 points for a study.[35] Therefore, we compared energy values for integration grids ranging from 40 × 40 grid to a 90 × 90 grid and found that the smallest grid gave the same value as the larger grid for this highly symmetrical ion. Isodensity values of 0.0004 au (0.25 kcal/mol)[35,38] or 0.001 au[36] have been suggested as providing a reasonable representations of molecular volume over a practical range of 0.0004−0.002 suggested by a study of many isomerization free energy differences.[36] We compared a range of isodensity values for $V(CO)_6^-$ modeled by DFT (B3LYP) and basis sets of 6-311G(d,p) for C and O and 6-311G for V, which have been shown to provide reasonable vibrational frequencies and bond distances.[17] The solvation stabilization energy by the IPCM method was 35.50, 36.41, 37.10, and 37.66 kcal/mol for isodensity values of 0.0004, 0.0007, 0.001, and 0.0013 au, respectively. The difference between 0.0004 and 0.001 au was 1.60 kcal/mol, which is a 4.5% increase in energy of solvation. The cavity size parameter appears to be a small effect within a range that previously has been used to provide good results for computing differences in solvation free energy.[36]

The potential curve for the ion pair was generated by keeping the internal geometry of the cation and anion at their gas-phase values and then moving the coordinates to create a desired metal separation distance for a given symmetry. A similar procedure was used for the radical pair. The IPCM method was used with isodensity defined at 0.0004 au and a dielectric constant for

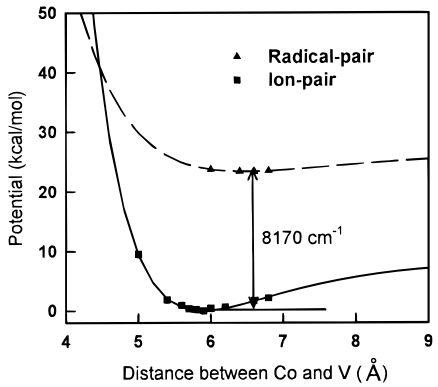

Figure 6. Solvation calculation by the isodensity polarized continuum method (IPCM) and DFT methods for the ion pair $Co(Cp)_2^+|V(CO)_6^-$ and a neutral pair. The method was similar to Figure 5, where the individual geometry was held fixed at a given metal separation.

DCM of 8.93 with a surface integration grid of 60 × 60 in the angle increments. The resulting total energies of the pairs are shown in Figure 6, where we plot relative energies normalized to the minimum energy for each pair. The separated ions are not used as a reference point since the solvation calculation is not absolute. If we examine Figure 6 we see that an energy gap of 8170 cm^{-1} is found between the minimum of the solvated ion pair and radical pair. In the solvated ion pair case we fit the potential energy to a Morse potential and obtained 35 cm^{-1} for the first vibrational level. The experimental energy gap is not known, but we have some idea based on redox potentials from electrochemistry in acetonitrile solvent,[12] where the $E_{1/2}$ values are 0.95 V for cobalticium cation and −0.06 for $V(CO)_6^-$. The difference of these values, 8146 cm^{-1}, corresponds to the energy separation of isolated ions in a more polar solvent like acetonitrile, so that both a correction for dichloromethane and a bond energy would be required to make a precise comparison. We can surmise that a value around 8000−10 000 cm^{-1} would be reasonable.

The solvation energy was tested for its sensitivity to specific isodensity values. The absolute solvation energy of the ion pair was increased by 974 cm^{-1} when the isodensity energy was increased from 0.0004 au to 0.001 au. However, the energy gap difference between radical pair and ion pair was 8461 cm^{-1} for the 0.001 isodensity value, or an increase of only 287 cm^{-1} or 3.5%. The calculated value of the energy gap is not used directly, since we fit the absorption spectrum to obtain the energy gap consistent with calculation and data. However, the reasonable value for this energy gap and its low sensitivity to specific isodensity values gives strong support to using the IPCM model to estimate the solvent reorganization energy for the excitation from ion pair to radical pair. This value is difficult to obtain independently, so a reasonable estimate is important for our data analysis. As we shall see, *our conclusions are not sensitive to knowing this value very accurately*.

A number of methods for computing solvent reorganization energies are available. The simplest methods use dipole moments and elliptical shapes to provide estimates.[39−41] In recent work, progress has been made on the computation of reorganization energy with both semiempirical and ab initio quantum chemistry codes. In particular, within a given continuum solvation model one can take the energy difference between the desired dielectric constant and the infinite frequency dielectric constant for each state and then take the difference of these results to provide the reorganization energy.[42] Within this framework, conceptually similar to early work,[39] there still remains the choice of particular electrostatic models.[36] Other approaches to computing reorganization energy are molecular theories[43,44] and theories that add another parameter to deal with possible frequency effects[45−47] in solvent reorganization. This field is evolving, and as more incisive comparisons of experiment and theory become available there will be more definitive guidelines for choosing different computational approaches. For the case of large systems, more diffuse charge density of the solute, and lower dielectric solvents we expect that the simpler continuum model of IPCM with realistic molecular shapes can be successful for computing the reorganization energy by the method of double differences.[42]

We computed the total energy for the ion pair and radical pair at their respective minimum energy distances of 5.9 and 6.6 Å with dielectric constants of 8.9 and 2.0 at an isodensity of 0.0004 au. The solvent reorganization energy is 3020 cm^{-1} for this case, which is a large fraction of the energy gap. We provide a check on the sensitivity of this value to specific isodensity assumptions by repeating the calculation for an isodensity of 0.001 au. We find a reorganization energy value only 1% larger. The value of 3020 cm^{-1} is reasonable if compared with a rough estimation method that assumes a full charge movement at the distance of 5.9 Å and an elliptical solvation model.[40] This model predicts about 4700 cm^{-1}; however, the ellipse is not a good model for our ion pair so the energy is very dependent on ellipse parameters. The IPCM computed dipole moment in DCM solvent is 26.7 D at 5.9 Å, which is similar to the 28.3 *D* value from a full charge displacement. These dipoles suggest that a model for the charge movement is approximately given by using the metal−metal distance and a full unit charge transfer. The identification of the actual amount of charge transfer has become an important diagnostic, especially for bimetallic complexes unlike our molecule, where covalent bridges serve to often restrict charge movement to the bridging molecule rather than fully between the metals. In particular, Stark effect measurements have been useful at demonstrating much smaller actual dipole moment changes in bimetallic complexes.[48−51] The application of these data within a generalized Mulliken−Hush model[52,53] has allowed extraction of interaction matrix elements for these types of systems.

D. Vibrations of $Na^+|V(CO)_6^-$. Since the ion pair complex is too complicated to easily optimize the geometry, the simpler complex $Na^+|\ V(CO)_6^-$ was geometry optimized with two different symmetries by DFT methods. The goal is to examine intensities and polarizations for vibrations of distorted $V(CO)_6^-$ to support our prediction of geometry for $Co(Cp)_2^+|V(CO)_6^-$. One geometry is for C_{3v} symmetry, with Na in contact with three oxygen atoms, which is similar to the top-triple contact model in the $Co(Cp)_2^+|V(CO)_6^-$ ion pair. Another structure has C_{2v} symmetry, where the Na is contacted with two oxygen atoms, similar to the side-double contact model for $Co(Cp)_2^+|V(CO)_6^-$. The parameters for the optimized geometry are shown in Table 4.

We see that $V(CO)_6^-$ is greatly distorted in both cases, as expected for a gas-phase interaction with such a small cation. The triple-contact model is slightly more stable than the double-contact model by about 2 kcal/mol, calculated by DFT with the B3LYP method and basis sets of 6-31G* for C, O and 6-311G for metals. The vibrations of these two models were calculated and IR/Raman intensities were predicted from the Gaussian 98W program.[33] For vibrations, the basis sets for C and O were 6-311G(d,p) in the double-contact geometry or 6-31G* in the triple-contact geometry. Table 5 shows the calculated relative Raman intensity and depolarization ratio of

TABLE 4: Geometry of $Na^+|V(CO)_6^-$ by DFT (B3LYP)[d]

	C_{2v}	C_{3v}
R(C−O)[a,b]	1.15792, 1.15212, 1.19520	1.18556, 1.15185
R(V−C)[a,b]	1.90192, 2.01357, 1.97713	2.01265, 1.91551
R(V−Na)[a,b]	3.85787	3.5425
	80.56, 94.80, 89.45, 90.62,	92.89, 81.20, 171.91
∠(C−V−C)[c]	178.38, 172.88, 172.88	
∠(O−C−V)[c]	168.28, 177.65, 177.72	177.84, 163.33

[a] The bond lengths are in ångstroms. [b] The oxygen atoms that have the longest C−O bond lengths are closest to the Na atom, while the carbon atoms that have the shortest V−C bond lengths are closest to the Na atom. [c] The angles closest to the Na atom are the smallest. The angles are in degrees. Notation for angles is ∠(ABC) where atom B at the vertex. [d] Gaussian 98W (6-31G* basis for C and O, 6-311G for V and Na).[33]

the vibrational modes of $V(CO)_6^-$ with O_h symmetry and two different complexes of $Na^+|V(CO)_6^-$. While the actual ion pair in the solvent has a much weaker interaction and does not have the degree of frequency change as shown for this complex, we use the predicted Raman intensities for highly distorted anions as a guide to the effects of distortion.

The O_h geometry of free $V(CO)_6^-$ shows computed intensities and polarizations that are in reasonable agreement with experiment for the high-frequency CO stretching modes, where we find a polarized A_{1g} mode, υ_1, and a depolarization value of 0.75 for the E_g mode, υ_3. There is a difference between experiment and prediction for the M−C mode, υ_4, at 393 cm^{-1}, where the predicted value is 0.75 but we observe 0.49. We also note that in THF solvent (Table 1) this mode showed values of 0.72, which is closer to expectation. Since most of the experiments on O_h geometry are for DCM solutions with Na^+ and diglyme, we could also have weak complexation effects leading to slight distortions. Experimentally, the IR active υ_6 mode also shows very weak Raman scattering, possibly from Na^+ interactions in solution.

For $Na^+|V(CO)_6^-$ there is a large difference between C_{3v} and C_{2v} symmetry for the depolarization ratio of the υ_1 mode. We note from Table 5 that the C_{3v} symmetry structure has a small depolarization ratio of 0.099, despite significant geometric distortion, while the C_{2v} symmetry has a value of 0.745. The 0.099 depolarization suggests that this symmetry of complexation will have less effect on the υ_1 mode than the C_{2v} geometry. In the Raman experiments, the υ_1 mode for the $Co(Cp)_2^+|V(CO)_6^-$ complex showed a significant nonzero value of 0.26, and since the frequencies are similar to free $V(CO)_6^-$, this must derive from slight geometric distortions from octahedral symmetry. Recall that we compute a side-bonded geometry as most stable for this complex, which should provide small distortions similar to those larger distortions in the C_{2v} case of $Na^+|V(CO)_6^-$. If the depolarization is not too sensitive to the magnitude of the distortion, then the larger depolarization of C_{2v} $Na^+|V(CO)_6^-$ supports the computed side-bonded geometry for $Co(Cp)_2^+|V(CO)_6^-$.

Additional calculations are needed for weaker interacting cations to confirm that the depolarization effect is clearly associated with υ_1 in the C_{2v} geometry. Ultimately, a complete model of the ion pair complex with fully optimized geometry may be essential for discussing more subtle features of the Raman intensities and polarization. Preliminary examination of this problem suggests that modest C_{2v} distortions are likely.

IV. Analysis of Data

Resonance Raman spectroscopy has been a very important spectroscopic technique for studying the structure and dynamics of both ground and excited states of molecules in both gas and solution phases.[54,55] Several groups[55−57] have summarized how to obtain dynamical information and geometric distortion in excited states from resonance Raman spectroscopy. According to time-dependent theory,[55−60] the Raman scattering cross-section is related to the excited state dynamics that arises from geometric displacements between the two states. The relative displacement of vibrational modes can be related to the relative intensities in the resonantly enhanced Raman spectrum, and this takes a particularly simple form when the dephasing rate is fast (line broadening is large). The fitting of absorption spectra has become a standard technique in extracting absolute bond length changes from resonance Raman spectra.[55−57] Particularly relevant to our case are applications to charge-transfer complexes.[61−63]

We follow the methods of prior workers in fitting absorption spectra to obtain absolute bond displacements, where the energy gap (E_{00}) and the solvent reorganization energy (λ_s) are parameters in the fit. Ultimately, the self-consistent fit to the absorption spectrum leads to a near constant sum of E_{00} and the solvent reorganization energy, λ_s, so that knowing one parameter helps define the other. The method has ambiguity for charge-transfer molecules, where the absorption spectrum has no structure and is very broad. Since the solvent reorganization energy is a major broadening feature, and its value is difficult to obtain experimentally, prior workers have obtained the reorganization energy from models of line broadening. Models for solvent broadening have been extensively discussed in the literature,[8,63] and solvent broadening mechanisms lead to either a single empirical parameter model or a two-parameter Brownian oscillator model.[64] In our absorption spectrum, we have overlap with higher energy transitions, so fitting to both sides of the absorption band edges is not possible. With large reorganization energy and a very broad absorption band of this type, an absorption spectrum fit cannot provide much more than a reasonable estimate of electronic energy gap and approximate values of bond displacements. Therefore, our strategy for using absorption spectra has been to confirm that computed bond length estimates and selected Raman enhancement data are self-consistent while assuming a computational value of solvent reorganization energy. Since one mode has large Raman enhancement and only two other modes have significant contributions, we iterate those values while assuming computational results for minor vibrational mode contributions.

In fitting the absorption spectrum, the four totally symmetric vibration modes that we detected and the internal vibration between $Co(Cp)_2$ and $V(CO)_6$ could be used to define the displacements. The observed vibrations of the $Co(Cp)_2^+|V(CO)_6^-$ ion pair obtained by resonance Raman spectroscopy are summarized in Table 1, where υ_1, υ_2, υ_4', and υ_3' are the totally symmetric modes. The data fitting and intensity analysis show that, relative to the V−C stretch (υ_2, 373 cm^{-1}) the totally symmetric C−O stretch mode (υ_1, 2020 cm^{-1}) was enhanced by 28 times and the Co−Cp vibration (υ_4', 315 cm^{-1}) was enhanced by about 1.3−1.7 times. The Cp ring breathing mode (υ_3', 1114 cm^{-1}) and other vibrations showed no obvious enhancement.

The calculations in Table 2 show that for $Co(Cp)_2$ there is little change of C−C and C−H bond between the ion and radical, so υ_1' and υ_3' should not be obviously enhanced. However, there are relatively large changes of V−C and Co−Cp distances. Since these displacements involve the υ_4' (Co−Cp stretch, A_{1g}) and υ_2 (V−C stretch, A_{1g}) vibrations, and there is no large enhancement of these low-frequency modes, fast excited state relaxation dynamics is likely for this system. The apparent reduction of enhancements for low-frequency modes

TABLE 5: Calculated Raman Frequency, Intensity, and Depolarization Ratio for the Vibrations of $V(CO)_6^-$ (O_h Symmetry) and $Na^+|V(CO)_6^-$ (C_{3v} and C_{2v}) by DFT(B3LYP)[e]

O_h				C_{3v}				C_{2v}			
mode[a]	R[b]	IR[c]	D[d]	mode[a]	R[b]	IR[c]	D[d]	mode[a]	R[b]	IR[c]	D[d]
382 (A_{1g})	73	0	0	A_1, 367	42	22	0.001	A_1, 360	44	25	0.030
389 (E_g)	38	0	0.75	E, 391	16	11	0.75	A_1, 375	21	0.1	0.218
								B_2, 393	5	7.5	0.750
1954 (T_{1u})	0	7833		E, 1844	66	2176	0.75	B_2, 1769	28	1218	0.750
				A_1, 1920	44	2291	0.07	A_1, 1831	201	2204	0.143
								B_1, 2014	6	2254	0.750
1974 (E_g)	500	0	0.75	E, 2078	426	68	0.75	A_1, 2044	281	313	0.744
								B_2, 2064	237	1009	0.750
2084 (A_{1g})	38	0	0	A_1, 2132	36	487	0.099	A_1, 2121	79	439	0.745

[a] The frequency in cm^{-1} for the vibrations of $V(CO)_6^-$. [b] Absolute Raman Intensity. [c] Absolute IR intensity [d] Depolarization ratio $D = I_{perpendicular}/I_{parallel}$. [e] Gaussian 98W, (6-311G(d,p) basis for C and O, 6-311G for V and Na).[33]

and the significance of large damping factors in the time dependent theory have been previously discussed in the literature.[55−57] When the damping factor is large we can simply obtain the relative displacement of the totally symmetric modes υ_1 and υ_2 from their relative Raman enhancement. Formulas are given in the literature[56,57] for converting dimensionless displacement Δ into normal coordinate change ΔQ (Å) and obtaining the internal coordinate changes (Δq) from the normal coordinates (Q).[57]

The potential energy calculation of Figure 6 shows that there is a weak bond between $Co(Cp)_2$ and $V(CO)_6$ with a very low vibrational frequency. For the solvated ion pair we fit the potential energy to a Morse potential where the first vibrational level is only 35 cm^{-1}, while the gas-phase potential gives 76 cm^{-1}. The upper surface of the radical pair is very flat, and any weak interaction would give a negligible frequency compared with the ion pair. Even though an inter-radical vibration of such a low frequency will not be important in our rate models (see next section), a low-frequency mode is useful to include in the rate model to provide improved frequency matching. A candidate totally symmetric mode of 84 cm^{-1} is present in the radical $V(CO)_6$, which can be related to $V(CO)_6^-$ if we consider it as slightly distorted from an octahedron. Therefore, we used a value of 84 cm^{-1} to examine its significance in our fit to the absorption spectrum. The fitting results show that this mode is not significant when its dimensionless displacement changes from 0 to 1.

The method of fitting the absorption spectrum only varied displacements of three modes and used calculations for the other modes. The displacements of the υ_4', υ_2, and υ_1 modes, which calculation predicts to have large displacements, are fitted to the absorption spectrum while keeping the relative displacement ratios. Calculations show that there are small coordinate changes of υ_1' (C−H stretch), υ_3' (Cp ring breathing), and υ_2' (CH bending), consistent with little enhancement for these modes in resonance Raman spectra. We used the calculated displacements for these modes and added υ_{11} (84 cm^{-1}) for a low-frequency mode, as discussed above. We used the IPCM calculation result of 3020 cm^{-1} for λ_s, a large damping factor of 1000 cm^{-1} and a zero energy of 10 420 cm^{-1} to fit the absorption spectrum. The displacements of the involved modes are listed in Table 6. We found that the fitting quality of the long wavelength side in the absorption spectrum depended on the displacement of υ_1, so that we could get a reasonable displacement for this mode, which defines the displacement of υ_2. The displacement of υ_4' was also varied, and it was sensitive to the edges of the absorption spectrum. A different solvent reorganization energy would shift the zero energy; however, it does not affect the vibrational displacements. For example, if we used the solvent reorganization energy of 4700 cm^{-1} that we obtained from elliptical models, the corresponding zero energy is 8700 cm^{-1} with the same displacements listed in Table 6. Similarly, a solvent reorganization energy of 3800 cm^{-1} requires a zero energy of 9600 cm^{-1}, consistent with the idea that the sum of these two values is about 13 400 cm^{-1}.

TABLE 6: Vibrational Displacement of the Ion Pair by Fitting of the Absorption Spectrum

		internal coordinate change (Δq)	
mode[a]	Δ[b]	fit[d]	calc[c]
υ_{11} (84 cm^{-1})	0.5	−	0.0625
υ_4' (315 cm^{-1})	1.35	0.0387	0.089
υ_2 (373 cm^{-1})	1.55	0.0508	0.0519
υ_3' (1114 cm^{-1})	0.1	−	0.00122
υ_1 (2020 cm^{-1})	1.38	−0.0199	−0.0175
υ_1' (3100 cm^{-1})	0.01	−	−0.000544

[a] υ with prime represents the vibrations in $Co(Cp)_2^+$ and, without prime, $V(CO)_6^-$. [b] Dimensionless displacement. [c] Calculation in angstroms. [d] Three frequencies were iterated and calculation results were used for the other modes.

Table 6 shows that the results of the fit are consistent with the calculation results, except for υ_4', whose displacement is smaller than the calculated prediction. This calculation was for a lower basis quality than for vanadium carbonyl, so perhaps this is a factor since metal bonding distances are sensitive to basis set and DFT method. More computations will be required to check this point. However, we also tried a two-parameter Brownian oscillator model[64] where we fix the reorganization energy to define self-consistent parameters. A variety of fits are possible with this model that give displacements for υ_4' closer to theory, but in most cases the parameters do not meet the internal assumptions of the Brownian oscillator model.

In summary, the geometry changes obtained from fitting Raman enhancements and the absorption spectrum are in satisfactory agreement with computational predictions. The broad absorption spectrum is less useful in refining displacements of low-frequency vibrations, but it is adequate for confirming the displacement of the totally symmetric, carbonyl stretching vibration and for defining a reasonable energy gap. These results limit the possible values for key molecular displacement parameters, which are needed for computing Franck−Condon factors in the rate models described in the next section.

V. Electron Transfer Rate Predictions

The rate of ET can be predicted with a quantum model for weakly coupled ET rates when the molecular data from the

above sections is combined with theory. In previous work from this lab[7] we used a model for rate constants that made predictions of quantum resolved rate effects, and this model is applicable here since we have good values for geometry changes and estimates of electronic coupling from the charge-transfer absorption band. Our goal is to see if the absolute rate constant is consistent with the data and if the observed changes in ET rate with vibrationally resolved quantum state are predictable. The model is a simple product of electronic factor and sum over Franck−Condon Factors that give energy matching.[65−67]

The model uses a coupling matrix element of 417 cm^{-1}, vibrational displacements as given in Table 6, an energy gap of 10 420 cm^{-1} and a solvent reorganization energy of 3020 cm^{-1}. The six modes shown in Table 6 were used to calculate the rate, where we used the dimensionless displacements listed in the second column. The radical frequencies were estimated as 84, 373, 315,1114 and 3100 cm^{-1}; they were used as acceptor modes with Franck−Condon factors that only include geometry changes. The totally symmetric mode is 2020 cm^{-1} for the ion and 2096 cm^{-1} for the radical, where both geometry and frequency effects are used in the FCF. This mode serves as an optical mode (as well as acceptor mode) so that rates for different quantum populations in this CO stretching mode can be computed and used as representing the maximum possible quantum effect in this model. As shown in prior simulations,[7] for a large energy gap case only a vibration with large FCF for changing quantum numbers between states can provide a dependence on initial quantum number. The high-frequency infrared active mode has no geometry change because of its symmetry, and no significant frequency change in the absence of Duschinsky[68] mode mixing. These properties of the infrared active CO stretch give small FCF for changing quantum numbers between states so that this vibration makes little contribution to the FCF sums that define the ET rate. Vibrations with such a small contribution to the rate will not give an ET rate dependent on the initial quantum population. The experimental results were 26.4, 11.3, and 5.5 ps for the $\upsilon = 0$, 1, 2 vibrational levels of the infrared active mode.[6]

The predictions of the model give ET lifetimes ($1/k$) for the quantum numbers $\upsilon = 0$, 1, 2, and 3 of 0.192, 0.087, 0.063, and 0.058 ps, respectively. This predicts a significant quantum effect of $k_1/k_0 = 2.2$ and $k_2/k_1 = 1.4$ for the totally symmetric vibration. The values show a 135 time shorter lifetime than observed for the $\upsilon = 0$ level (26 ps). The model shows that the total vibrational reorganization energy of $\lambda_v = 2747$ cm^{-1} had a contribution from the 2096 cm^{-1} optical mode of $\lambda_1 = 1996$ cm^{-1}, the 373 and 315 cm^{-1} modes had $\lambda_2 = 448$ and $\lambda_{4'} = 287$ cm^{-1}, and the other modes had small energies $\lambda_i < 11$ cm^{-1}.

We investigated the sensitivity of these predictions to the specific values of the energy gap and solvent reorganization energy. Since the fitting of the absorption spectrum is a more sensitive test of the sum of these values rather than each value, we can arbitrarily pick new reorganization energies and gaps (sum of 13 420 cm^{-1}) to check the sensitivity of predicted values to this computed parameter. For reorganization energies of 2220, 2620, 3020, 3420, 3820, 4220, and 4620 cm^{-1} we found lifetimes for $\upsilon = 0$ of 0.605, 0.329, 0.192, 0.118, 0.078, 0.055, and 0.042 ps. These values show that a reorganization energy value of 2220 cm^{-1} would be required to make the predicted rate only 43 times faster than observed, while the larger reorganization energies have much larger ET rates. The quantum effect k_1/k_0 for the totally symmetric mode υ_1 at these same reorganization energy values is 3.02, 2.59, 2.20, 1.82, 1.47, 1.16, and 0.88, while k_2/k_1 values are 1.82, 1.59, 1.39, 1.18, 0.99, 0.82, and 0.67, respectively.

We believe that the solvent reorganization energy is not likely to be lower than 2620 cm^{-1}, which is about 2100 cm^{-1} below the prediction of a classical elliptical model and 420 cm^{-1} below our computed value of 3020 cm^{-1}. Therefore, we conclude that the model predicts an ET rate that is about 79−135 times faster than actually observed for $\upsilon = 0$ for solvent reorganization energies of 2620−3020 cm^{-1}. Furthermore, the observed infrared active mode should not have a quantum effect while the totally symmetric mode could have a reasonably large quantum effect for k_1/k_0 and less effect for k_2/k_1.

We conclude that standard ET theory in the weak coupling limit provides an incorrect magnitude for the ET rate. In addition, only totally symmetric CO stretching modes are capable of having a quantum effect on the ET rate in the standard rate expression.

VI. Discussion of Predictive Failure

A. Magnitude of Rate. The prior sections have used resonance Raman data, absorption spectra, and computational models to define both electronic coupling and vibrational distortions appropriate for ET rate calculations. The ET rate was predicted to be 135 times faster than observed, which suggests a major failure in the assumptions. The key assumption in the "standard" model is that no important changes in the upper electronic surface occur after the absorption event. Absorption spectra and Raman spectra are "vertical" processes that probe instantaneous features of the potential surface. However, if relaxation of the upper state geometry dramatically changes the overlap of electronic wave functions, then the electronic overlap inferred from the absorption spectrum and the computed electronic coupling of 417 cm^{-1} could be very wrong. We believe that this is the reason for the rate being much slower than the prediction. However, if future computations do not demonstrate the 11.6 times lowering of the coupling matrix element needed to account for the 135 reduction in rate, then we need to assess the validity of the weak coupling implied in the "standard" model. Very recently, a prediction of the effects of increased coupling has been made for charge-transfer complexes that shows a slowing of electron-transfer rate as the coupling increases beyond the weak coupling limit.[69] This type of model needs study for our particular system, but it suggests that the weak coupling model may only be applicable to coupling matrix elements significantly smaller than k_BT, which is 210 cm^{-1} for our experiments.

The negligibly small vibrational frequency changes for $V(CO)_6^-$ between free solution and the ion pair suggests that geometric distortions are small, even though the depolarization implies distortion from the octahedral geometry. We often discuss the vibrational spectrum of individual species, but the electronic state is of the complete ion pair so that the overall symmetry is low. For example, if we consider the distortions of $V(CO)_6^-$ in the ion pair in the side-bonded, double-contact geometry, it is likely that locally the highest possible symmetry is C_{2v} where CO movements can easily reduce this to C_2. These deviations from O_h undoubtedly lift all vibrational degeneracy, but with broad solvent widths the small shifts from lifting degeneracy are not observed in the spectrum. Upon excitation to the neutral radical pair the ionic interaction between the two parts of the pair is removed and the geometry of the $V(CO)_6$ radical might be expected to be more similar to its free structure. However, the $V(CO)_6$ radical is Jahn−Teller perturbed so that low-energy structures different from D_{3d} are sampled by a small

activation energy so that even weak interaction with $Co(Cp)_2$ may still be sufficient to stabilize one geometry. If we reduce the $V(CO)_6$ radical symmetry by interaction, then we remove the g,u symmetry labels and there are many low-frequency motions that can interchange different structures. In this case the electronic interaction between the radicals is also fluctuating, and we expect optimal wave function overlap with the $Co(Cp)_2$ species when the structure approaches O_h character. This overlap dependence upon geometry occurs because the electronic orbital involved in the ET is mostly metal localized and the degree of delocalization onto the oxygens depends on the geometry. A graphical representation of orbitals suggests that the orbital overlap is reduced in the radical pair. However, theoretical calculations are required to examine the argument quantitatively, and this approach will be investigated soon.

B. Origin of Quantum Rate Effect. The quantum effect observed in the experiments with the IR active CO stretching mode is not predicted from the calculation, since only a totally symmetric CO stretching mode with a large geometry change can have large Franck−Condon Factor effects in the simplest rate models. In the experimental data for $V(CO)_6^-$ and in the normal mode computations for the $V(CO)_6^-$ and $V(CO)_6$ vibrations the symmetric stretch vibration is about 100 cm^{-1} higher in frequency than the IR active mode. This large frequency offset and weak IR absorption suggests that the experimental probe was not inadvertently monitoring the totally symmetric mode. Consequently, the first issue to understand is how the IR active CO stretching mode is populated, and then how its quantum number can affect the ET rate.

The population of IR active CO stretching modes must occur via an intramolecular vibrational relaxation (IVR) mechanism. Solvent collisions can serve to create energy and momentum matching conditions for converting totally symmetric motions into an IR active motion either directly or in combination with other very low-frequency vibrations. There is some literature on IVR in metal carbonyls[70] that shows a T_{1u} IR pumped mode in $W(CO)_6$ relaxing to the E_g mode but not to the A_{1g} mode in CCl_4 solvent. The relaxation time scale[71] is 10−20 ps in similar IR pumping experiments that do not monitor the final state population. These results suggest that coupling to A_{1g} modes is not significant, at least in some solvents for high-symmetry, closed-shell molecules. In our case, the optical Franck−Condon factors are creating population in totally symmetric motions in combination with other low-frequency motions that are thermally populated. The initial radical geometry is Jahn−Teller unstable so that relaxation must occur to a different symmetry. Therefore, it is likely that coupling between totally symmetric and nontotally symmetric CO stretching modes can occur during or after this geometric relaxation. The electronic-vibrational coupling implied in the Jahn−Teller relaxation might be effective in enhancing the conversion of totally symmetric to nontotally symmetric motions. In addition, solvent collisions can provide asymmetric forces or instantaneous normal modes.[72−74] The time scale for conversion to IR active CO modes is of interest, and experimentally we have reduced the time resolution to below 250 fs to measure this quantity. One might find such a conversion occurring very rapidly as part of the initial low-frequency distortion or happening somewhat later. The mechanical view of such a conversion would suggest that the time scale might involve hundreds of femtoseconds to convert from a totally symmetric motion to a mode that looks like an IR active absorption with CO motions out of phase. The temperature dependence is of interest, since nontotally symmetric vibrations might be important in the conversion.

While the IVR mechanism is most attractive for populating nontotally symmetric vibrations, such coupling of CO stretching motions could persist for times long after the initial pumping and relaxation event rather than being a unidirectional transformation linked to the geometry change. This strong coupling mechanism could lead to statistical populations of each type of high-frequency vibration in an IVR pool of all high-frequency vibrations. If this were possible, then the observed population in the IR active modes could be accompanied by a "hidden" population in the other CO motions. Since we predict a quantum effect for the totally symmetric mode, the "hidden" population in this mode might become the source of a quantum effect for the IR active mode.

We examined a statistical IVR pool model to check if the observed quantum effect is likely to originate from "hidden" populations in the totally symmetric mode. From our modeling of the absorption band we note that the excitation wavelength near 600 nm is pumping combination bands containing C−O totally symmetric motions mostly in the $\upsilon = 1$ quantum level, but with some $\upsilon = 2$ at lower probability. We formulated a statistical model for spreading the initial quanta in the totally symmetric C−O stretching mode into all possible C−O stretching modes with conservation of quanta. We used a degeneracy of 3 for the IR mode, 1 for the totally symmetric mode, and 2 for the other high-frequency mode and then used Boson statistics to define the statistical probability for every possible individual state composed of different quantum numbers in these three modes. We assumed purely statistical populations. This yields the largest possible effect since equal statistical weighting of the different vibrational frequencies rather than Boltzmann weighting emphasizes population in the highest frequency, totally symmetric vibration. For example, when starting with two quanta in the totally symmetric mode each individual final state could have zero to two quanta in any of the three modes, which leads to a number of possible states. A prediction of average rate is desired for an observable defined by a specific quantum number in the IR mode. Therefore, the average rates were computed by forming a weighted average over all individual states having a specific quantum population in the IR active mode. Each individual state that has the desired quantum number in the IR active mode contributes to the average rate by multiplying its statistical probability (the weight) times a rate defined by the quantum number in the totally symmetric mode. The ET rate for the totally symmetric mode is obtained from the computations discussed previously, where $\upsilon = 1$ and $\upsilon = 2$ were 2.20 and 3.05 times larger than the $\upsilon = 0$ rate.

With this method of calculation the main unknown is the initial distribution of population in the totally symmetric mode. Therefore, the relative amount in $\upsilon = 1$ versus $\upsilon = 2$ from the optical pumping of the totally symmetric CO stretching vibrations was varied to have the amount in $\upsilon = 1$ either 0.5 or 2 times the $\upsilon = 2$ case. To achieve a maximum in the predicted effect, we ignored any initial optical pumping into $\upsilon = 0$. The model shows a maximum increase of 30% in rate for $\upsilon = 1$ in the IR active mode, but this also would have a decrease in rate of a factor of 3 by going to $\upsilon = 2$. These results suggest that the "hidden" population in the totally symmetric mode cannot explain the quantum effect observed in the experimental measurement of IR populations, which had about a 2-fold increase per additional quantum of population. In general, uniform statistical relaxation out of a singly degenerate state with totally symmetric character dilutes any quantum effect caused by that mode unless there were very different relaxation

pathways for different numbers of quanta in the mode. While unusual mechanisms are possible, and they might be revealed by experiments pumping different parts of the absorption band, we tentatively feel that "hidden" populations in totally symmetric modes are not the source of the quantum effect on ET rate.

An additional consideration arises from geometry differences between the radical and ionic structures. A new geometry arising from a symmetry change requires that the vibrations in the initial state have a coordinate system different from that of the final state; in this case a given vibration in the initial state is a linear combination of vibrations in the final state. Spectroscopic observations involving a rotation and translation of the vibrational coordinate system have become known as Duschinsky effects.[68] We are systematically investigating the significance of such coordinate changes for ET and can provide a few remarks in the context of this system. The rate of ET is proportional to a sum of all Franck−Condon factors, which emphasizes any FCF effects that change the magnitude of the sum. For example, when some symmetry is preserved in the geometry change, a totally symmetric mode in the initial state might become a combination of all totally symmetric modes in the final state. *Since large frequency changes can provide Franck−Condon contributions, the inter-mixing of high and low frequencies in one state could provide large contributions to Franck−Condon factors.* This effect potentially enhances the contributions of totally symmetric vibrations in the presence of geometry changes, and it also *allows nontotally symmetric modes to become contributors to the sum of terms.* Currently, we are investigating these overlooked sources of important rate effects with model systems as well as for this particular system. Another aspect of the Duschinsky effect that only recently has been recognized is that the coordinate transformation can be nonlinear and nonorthogonal.[75,76] The consequences for ET have not been explored, but *this effect could provide another avenue for vibronic activity of nontotally symmetric modes*.

From the preceding analysis we conclude that the most likely cause of population in the IR active CO stretching mode is from IVR with a unidirectional conversion process from totally symmetric vibrations. The quantum effect in this mode is not from "hidden" populations of totally symmetric modes and must have another mechanism. We postulate that this mechanism could be due to breakdown of the Condon Approximation, which can have a difference in electronic coupling as a function of vibrational quantum number. Work is in progress computing these matrix elements, and preliminary results[77] show that this is a viable mechanism for having a quantum effect with the IR stretching mode.

Experimentally, the models suggest that temperature studies of rate could show effects if thermally populated modes are important for rate contributions by dynamic Jahn−Teller distortion. The rise time of infrared activity might reveal the IVR rate, while pumping at many places in the absorption profile can vary the fraction of any "hidden" populations of totally symmetric modes.

VII. Summary

This work has shown that standard models of electron-transfer cannot explain prior experimental results for the ion pair $Co(Cp)_2^+|V(CO)_6^-$. There is a large deviation in prediction for the absolute rate constant and the observed vibrational quantum effect on electron-transfer rates.

We analyzed new data for resonance Raman, absorption, and infrared spectra and combined these results with density functional (DFT) quantum calculations of structure, vibrational modes, and solvent effects to predict ET rates. Related DFT calculations on $Na^+|\ V(CO)_6^-$ are used to support a spectroscopic identification of the ion pair geometry. Solvation energies and solvent reorganization energies were calculated for both ion pairs and radical pairs with DFT and an isodensity polarized continuum model (IPCM). The resonance Raman and absorption spectra were combined with these DFT computations to provide a self-consistent set of molecular parameters for testing the "standard" assumptions of electronic transfer. Rate models for direct, weak coupling in the ion pair $Co(Cp)_2^+|V(CO)_6^-$ predict absolute ET rates that are ∼135 times too large for a coupling matrix element of 417 cm^{-1} inferred from the absorption spectrum. This deficiency probably is due to the assumption that the radical pair surface is adequately probed by data from resonance Raman and absorption spectra. From our DFT calculations on $Co(Cp)_2|V(CO)_6$ we conclude that a small geometry change in the upper surface relaxes the orbital populations via a Jahn−Teller effect and greatly reduces the electronic coupling for the return ET. This proposal is based on graphs of orbitals, and we plan quantitative comparisons of electronic coupling matrix elements to test this mechanism. If a reduction in matrix element cannot explain the results, we will need to evaluate the accuracy of the weak coupling rate model for our case.

The standard model also cannot explain the rate dependence of ET for quantum populations ($v = 0, 1, 2$) in the nontotally symmetric CO stretching mode that was probed by transient IR in prior work.[6] These rate effects are likely to involve a fast IVR conversion from totally symmetric vibrations to IR active CO stretching motions followed by ET. The alternative IVR hypothesis leading to a statistically populated pool of all CO stretching motions is not likely since a statistical analysis shows that "hidden" populations in totally symmetric vibrations cannot explain the observed data. Therefore, the vibrational quantum effect on ET is probably caused by a breakdown of the Condon approximation, which in our case requires that an increase in the quantum number of vibration also increase the coupling matrix element. Theoretical work is in progress and has tentatively confirmed a Condon breakdown for the IR active vibration.[77] We briefly discussed the possible importance of a Duschinsky effect in computing electron-transfer rates, and these mechanisms involving vibrational coordinate rotation and translation are under investigation.

Experimentally, the models suggest that temperature studies of rate could show effects if thermally populated modes are important for rate contributions by dynamic Jahn−Teller distortion. The rise time of infrared activity might reveal the IVR rate, while pumping at many places in the absorption profile can vary the fraction of any "hidden" populations of totally symmetric modes.

Acknowledgment. We thank the U.S. Department of Energy, Office of Energy Research, Division of Chemical Sciences (Grant DE-FG02-91ER14228) for support of this research.

References and Notes

(1) Newton, M. D.; Sutin, N. *Annu. Rev. Phys. Chem.* **1984**, *35*, 437.
(2) Marcus, R. A.; Sutin, N. *Biochim. Biophys. Acta* **1985**, *811*, 265.
(3) *Electron Transfer in Inorganic, Organic, and Biological Systems*; Bolton, J. R., Mataga, N., McLendon, G., Eds.; American Chemical Society: Washington, DC, 1991; p 295.
(4) Newton, M. D. *Chem. Rev.* **1991**, *91*, 767.
(5) Bixon, M.; Jortner, J. Electron transfer − From isolated molecules to biomolecules. In *Electron Transfer-From Isolated Molecules to Biomolecules*; John Wiley and Sons: New York, 1999; Part 1, Vol. 106, p 35.

(6) Spears, K. G.; Wen, X.; Zhang, R. *J. Phys. Chem.* **1996**, *100*, 10206.
(7) Spears, K. G. *J. Phys. Chem.* **1995**, *99*, 2469.
(8) Myers, A. B. *Chem. Phys.* **1994**, *180*, 215.
(9) Tominaga, K.; Kliner, D. A. V.; Johnson, A. E.; Levinger, N. E.; Barbara, P. F. *J. Chem. Phys.* **1993**, *98*, 1228.
(10) Hush, N. S. *Prog. Inorg. Chem.* **1967**, *8*, 391.
(11) To be published, Kenneth G. Spears.
(12) Bockman, T. M.; Kochi, J. K. *J. Am. Chem. Soc.* **1989**, *111*, 4669.
(13) Hartley, D.; Ware, M. J. *J. Chem. Soc. A* **1969**, 138.
(14) Abel, E. W.; McLean, R. A. N.; Tyfield, S. P.; Braterman, P. S.; Walker, A. P.; Hendra, P. J. *J. Mol. Spectrosc.* **1969**, *30*, 29.
(15) Stein, P.; Miskowski, V.; Woodruff, W. H.; Griffin, J. P.; Werner, K. G.; Gaber, B. P.; Spiro, T. G. *J. Chem. Phys.* **1976**, *64*, 2159.
(16) Reber, C.; Zink, J. I. *J. Phys. Chem.* **1992**, *96*, 571.
(17) Spears, K. G. *J. Phys. Chem. A* **1997**, *101*, 6273.
(18) Holland, G. F.; Manning, M. C.; Ellis, D. E.; Trogler, W. C. *J. Am. Chem. Soc.* **1983**, *105*, 2308.
(19) Keller, H. J.; Laubereau, P.; Nöthe, D. *Z. Naturforsch.* **1969**, *24*, 257.
(20) Rubinson, K. A. *J. Am. Chem. Soc.* **1976**, *98*, 5188.
(21) Boyer, M. P.; Page, Y. L.; Morton, J. R.; Preston, K. F.; Vuolle, M. J. *Can. J. Spectrosc.* **1981**, *26*, 181.
(22) Bratt, S. W.; Kassyk, A. K.; Perutz, R. N.; Symons, M. C. R. *J. Am. Chem. Soc.* **1982**, *104*, 490.
(23) Evans, S.; Green, J. C.; Orchard, A. F. *Chem. Phys. Lett.* **1969**, *4*, 361.
(24) Barton, T. J.; Grinter, R.; Thomson, A. J. *J. Chem. Soc., Dalton Trans.* **1978**, 608.
(25) Frisch, M. J.; Trucks, G. W.; Schlegel, H. B.; Gill, P. M. W.; Johnson, B. G.; Robb, M. A.; Cheeseman, J. R.; Keith, T. A.; Petersson, G. A.; Montgomery, J. A.; Raghavachari, K.; Al-Laham, M. A.; Zakrzewski, V. G.; Ortiz, J. V.; Foresman, J. B.; Cioslowski, J.; Stefanov, B. B.; Nanayakkara, A.; Challacombe, M.; Peng, C. Y.; Ayala, P. Y.; Chen, W.; Wong, M. W.; Andres, J. L.; Replogle, E. S.; Gomperts, R.; Martin, R. L.; Fox, D. J.; Binkley, J. S.; Defrees, D. J.; Baker, J.; Stewart, J. P.; Head-Gordon, M.; Gonzalez, C.; Pople, J. A. *Gaussian 94W*, version 2.1; Gaussian, Inc.: Pittsburgh, PA:, 1995.
(26) Riley, P. E.; Davis, R. E. *J. Organomet. Chem.* **1978**, *152*, 209.
(27) Hedberg, A. K.; Hedberg, L.; Hedberg, K. *J. Chem. Phys.* **1975**, *63*, 1265.
(28) Lippincott, E. R.; Nelson, R. D. *Spectrochim. Acta* **1958**, *10*, 307.
(29) Bodenheimer, J.; Loewenthal, E.; Low, W. *Chem. Phys. Lett.* **1969**, *3*, 715.
(30) Beck, W.; Nitzchmann, R. E. *Z. Naturforsch.* **1962**, *176*, 577.
(31) Schmidling, D. G. *J. Mol. Struct.* **1975**, *24*, 1.
(32) Bellard, S.; Rubinson, K. A.; Sheldrick, G. M. *Acta Crystallogr.* **1979**, *B35*, 271.
(33) Frisch, M. J.; Trucks, G. W.; Schlegel, H. B.; Scuseria, G. E.; Robb, M. A.; Cheeseman, J. R.; Zakrzewski, V. G.; Montgomery, J. J. A.; Stratmann, R. E.; Burant, J. C.; Dapprich, S.; Millam, J. M.; Daniels, A. D.; Kudin, K. N.; Strain, M. C.; Farkas, O.; Tomasi, J.; Barone, V.; Cossi, M.; Cammi, R.; Mennucci, B.; Pomelli, C.; Adamo, C.; Clifford, S.; Ochterski, J.; Petersson, G. A.; Ayala, P. Y.; Cui, Q.; Morokuma, K.; Malick, D. K.; Rabuck, A. D.; Raghavachari, K.; Foresman, J. B.; Cioslowski, J.; Ortiz, J. V.; Stefanov, B. B.; Liu, G.; Liashenko, A.; Piskorz, P.; Komaromi, I.; Gomperts, R.; Martin, R. L.; Fox, D. J.; Keith, T.; Al-Laham, M. A.; Peng, C. Y.; Nanayakkara, A.; Gonzalez, C.; Challacombe, M.; Gill, P. M. W.; Johnson, B.; Chen, W.; Wong, M. W.; Andres, J. L.; Gonzalez, C.; Head-Gordon, M.; Replogle, E. S.; Pople, J. A. *Gaussian 98*, Revision A.3; Gaussian, Inc.: Pittsburgh, PA, 1998.
(34) Tomasi, J.; Persico, M. *Chem. Rev.* **1994**, *94*, 2027.
(35) Foresman, J. B.; Keith, T. A.; Wiberg, K. B.; Snoonian, J.; Frisch, M. J. *J. Phys. Chem.* **1996**, *100*, 16098.
(36) Zhan, C. G.; Chipman, D. M. *J. Chem. Phys.* **1998**, *109*, 10543.
(37) Zhan, C. G.; Bentley, J.; Chipman, D. M. *J. Chem. Phys.* **1998**, *108*, 177.
(38) Wiberg, K. B.; Keith, T. A.; Frisch, M. J.; Murcko, M. *J. Phys. Chem.* **1995**, *99*, 9072.
(39) Marcus, R. A. *J. Chem. Phys.* **1956**, *24*, 966.
(40) Brunschwig, B. S.; Ehrenson, S.; Sutin, N. *J. Phys. Chem.* **1986**, *90*, 3657.
(41) Brunschwig, B. S.; Ehrenson, S.; Sutin, N. *J. Phys. Chem.* **1987**, *91*, 4714.
(42) Liu, Y. P.; Newton, M. D. *J. Phys. Chem.* **1995**, *99*, 12382.
(43) Perng, B. C.; Newton, M. D.; Raineri, F.; Friedman, H. L. *J. Chem. Phys.* **1996**, *104*, 7153.
(44) Perng, B. C.; Newton, M. D.; Raineri, F. O.; Friedman, H. L. *J. Chem. Phys.* **1996**, *104*, 7177.
(45) Basilevsky, M. V.; Chudinov, G. E.; Rostov, I. V.; Liu, Y. P.; Newton, M. D. *J. Mol. Struct.* **1996**, *371*, 191.
(46) Basilevsky, M. V.; Rostov, I. V.; Newton, M. D. *Chem. Phys.* **1998**, *232*, 189.
(47) Newton, M. D.; Basilevsky, M. V.; Rostov, I. V. *Chem. Phys.* **1998**, *232*, 201.
(48) Oh, D. H.; Sano, M.; Boxer, S. G. *J. Am. Chem. Soc.* **1991**, *113*, 6880.
(49) Karki, L.; Lu, H. P.; Hupp, J. T. *J. Phys. Chem.* **1996**, *100*, 15637.
(50) Bublitz, G. U.; Boxer, S. G. *Annu. Rev. Phys. Chem.* **1997**, *48*, 213.
(51) Brunschwig, B. S.; Creutz, C.; Sutin, N. *Coord. Chem. Rev.* **1998**, *177*, 61.
(52) Cave, R. J.; Newton, M. D. *Chem. Phys. Lett.* **1996**, *249*, 15.
(53) Cave, R. J.; Newton, M. D. *J. Chem. Phys.* **1997**, *106*, 9213.
(54) Clark, R. J. H.; Dines, T. J. *Angew. Chem., Int. Engl* **1986**, *25*, 131.
(55) Myers, A. B.; Mathies, R. A. Resonance Raman Intensities: A Probe of Excited-State Structure and Dynamics. In *Biological Applications of Raman Spectroscopy*; Spiro, T. G., Ed.; John Wiley & Sons: New York, 1987; Vol. 2, p 1.
(56) Zink, J. I.; Shin, K. S. K. Molecular Distortions in Excited Electronic States Determined from Electronic and Resonance Raman Spectroscopy. In *Advanced in Photochemistry*; Volman, D. H., Hammond, G. S., Neckers, D. C., Eds.; John Wiley & Sons: New York, 1991; Vol. 16, p 119.
(57) Myers, A. B. Excited Electronic State Properties from Ground-State Resonance Raman Intensities. In *Laser Techniques in Chemistry*; Myers, A. B., Rizzo, T. R., Eds.; John Wiley & Sons: New York, 1995; Vol. XXIII, p 325.
(58) Lee, S. Y.; Heller, E. J. *J. Chem. Phys.* **1979**, *71*, 4777.
(59) Heller, E. J. *Acc. Chem. Res.* **1981**, *14*, 368.
(60) Heller, E. J.; Sundberg, R. L.; Tannor, D. *J. Phys. Chem.* **1982**, *86*, 1822.
(61) Markel, F.; Ferris, N. S.; Gould, I. R.; Myers, A. B. *J. Am. Chem. Soc.* **1992**, *114*, 6208.
(62) Britt, B. M.; McHale, J. L.; Friedrich, D. M. *J. Phys. Chem.* **1995**, *99*, 6347.
(63) Myers, A. B. *Chem. Rev.* **1996**, *96*, 911.
(64) Li, B.; Johnson, A. E.; Mukamel, S.; Myers, A. B. *J. Am. Chem. Soc.* **1994**, *116*, 11039.
(65) Ulstrup, J.; Jortner, J. *J. Chem. Phys.* **1975**, *63*, 4358.
(66) Jortner, J. *J. Chem. Phys.* **1976**, *64*, 63.
(67) Brunschwig, B. S.; Sutin, N. *Comments Inorg. Chem.* **1987**, *6*, 209.
(68) Duschinsky, F. *Acta Physicochim. URSS* **1937**, *7*, 551.
(69) Wynne, K.; Hochstrasser, R. M. Coherence and Adiabaticity in Ultrafast Electron Transfer. In *Electron Transfer-From Isolated Molecules to Biomolecules*; John WIley and Sons: New York, 1999; Part 2, Vol. 107, p 263.
(70) Tokmakoff, A.; Sauter, B.; Kwok, A. S.; Fayer, M. D. *Chem. Phys. Lett.* **1994**, *221*, 412.
(71) Arrivo, S. M.; Dougherty, T. P.; Grubbs, W. T.; Heilweil, E. J. *Chem. Phys. Lett.* **1995**, *235*, 247.
(72) Kenkre, V. M.; Tokmakoff, A.; Fayer, M. D. *J. Chem. Phys.* **1994**, *101*, 10618.
(73) Ladanyi, B. M.; Stratt, R. M. *J. Phys. Chem. A* **1998**, *102*, 1068.
(74) Larsen, R. E.; Stratt, M. *J. Chem. Phys.* **1999**, *110*, 1036.
(75) Özkan, I. *J. Mol. Spectrosc.* **1990**, *139*, 147.
(76) Ruhoff, P. T. *Chem. Phys.* **1994**, *186*, 355.
(77) Private communication with Robert J. Cave and Newt Miller, Harvey Mudd College.